

Transformations between 2MASS, SDSS and BVI photometric systems for late-type giants

E. Yaz^{1,*}, S. Bilir¹, S. Karaali^{1,2}, S. Ak¹, B. Coşkunoglu¹, and A. Cabrera-Lavers^{3,4}

¹ Istanbul University, Faculty of Sciences, Department of Astronomy and Space Sciences, 34119 Istanbul, Turkey

² Beykent University, Faculty of Science and Letters, Department of Mathematics and Computer, Beykent, 34398, Istanbul, Turkey

³ Instituto de Astrofísica de Canarias, E-38205 La Laguna, Tenerife, Spain

⁴ GTC Project Office, E-38205 La Laguna, Tenerife, Spain

The dates of receipt and acceptance should be inserted later

Key words stars: late-type, stars: general, techniques: photometric

We present colour transformations from Two Micron All Sky Survey (2MASS) photometric system to Johnson-Cousins system and to Sloan Digital Sky Survey (SDSS) system for late-type giants and vice versa. The giant star sample was formed using surface gravity constraints ($2 < \log g \leq 3$) to Cayrel de Strobel et al.'s (2001) spectroscopic catalogue. 2MASS, SDSS and Johnson-Cousins photometric data was taken from Cutri et al. (2003), Ofek (2008) and van Leeuwen (2007), respectively. The final sample was refined applying the following steps: (1) the data were dereddened, (2) the sample stars selected are of the highest photometric quality. We give two-colour dependent transformations as a function of metallicity as well as independent of metallicity. The transformations provide absolute magnitudes and distance determinations which can be used in space density evaluations at relatively short distances where some or all of the SDSS magnitudes of late-type giants are saturated.

© 2010 WILEY-VCH Verlag GmbH & Co. KGaA, Weinheim

1 Introduction

The most widely used sky surveys are the Sloan Digital Sky Survey (SDSS; York et al., 2000) and the Two Micron All Sky Survey (2MASS; Skrutskie et al., 2006). SDSS is the largest photometric and spectroscopic survey in optical wavelengths, whereas, 2MASS has imaged the sky across infrared wavelengths. Another astrometrically and photometrically important survey is Hipparcos (ESA, 1997), which was reduced recently by van Leeuwen (2007).

SDSS obtains images almost simultaneously in five broad-bands (u , g , r , i and z) centred at 3540, 4760, 6280, 7690 and 9250 Å, respectively (Fukugita et al., 1996; Gunn et al., 1998; Hogg et al., 2001; Smith et al., 2002). The photometric pipeline (Lupton et al., 2001) detects the objects, matches the data from five filters and measures instrumental fluxes, positions and shape parameters. The magnitudes derived from fitting a point spread function (PSF) are accurate to about 2 per cent in g , r and i , and 3–5 per cent in u and z for bright sources (< 20 mag) point sources. Data Release 5 (DR5) is almost 95 per cent complete for point sources to $(u, g, r, i, z) = (22, 22.2, 22.2, 21.3, 20.5)$. The median FWHM of the PSFs is about 1.5 arcsec (Abazajian et al., 2004). The data are saturated at about 14 mag in g , r and i , and about 12 mag in u and z (see Chonis & Gaskell, 2008).

The near-infrared (NIR) JHK_s photometric data were taken from the digital Two Micron All-sky Survey¹ (2MASS). It provides the most complete database of galactic point sources available up to date. During the development of this survey, two highly automated 1.3-m telescopes were used: one at Mt. Hopkins, Arizona to observe the Northern sky, and the other at Cerro Tololo Observatory in Chile to complete the survey's Southern half. Observations cover 99.998 per cent (Skrutskie et al., 2006) of the sky with simultaneous detections in J (1.25 μm), H (1.65 μm) and K_s (2.17 μm) bands up to the limiting magnitudes of 15.8, 15.1 and 14.3, respectively. Nowadays, 2MASS is probably the reference study for the rest of galactic surveys, due to both full coverage of the sky which it provides and its intrinsic photometric and astrometric accuracies. Recent surveys, such as UKIDSS (Lucas et al., 2008), use 2MASS as reference catalogue, therefore a transformation between optical and 2MASS magnitudes is of interest in many different topics. The photometric uncertainty of the data is less than 0.155 at $K_s \sim 16.5$ magnitude which is the photometric completeness of 2MASS for stars with $|b| > 25^\circ$ (Skrutskie et al., 2006). Calibration offsets between any two points in the sky are less than 0.02 mag. The passband profiles for Johnson-Cousins, SDSS and 2MASS photometric systems are given in Fig. 1.

It has been custom to derive transformations between a newly defined photometric system and those that are more traditional (such as the Johnson-Cousins $UBVR_I$ system).

* Corresponding author: e-mail: esmayaz@istanbul.edu.tr

¹ <http://www.ipac.caltech.edu/2MASS/>

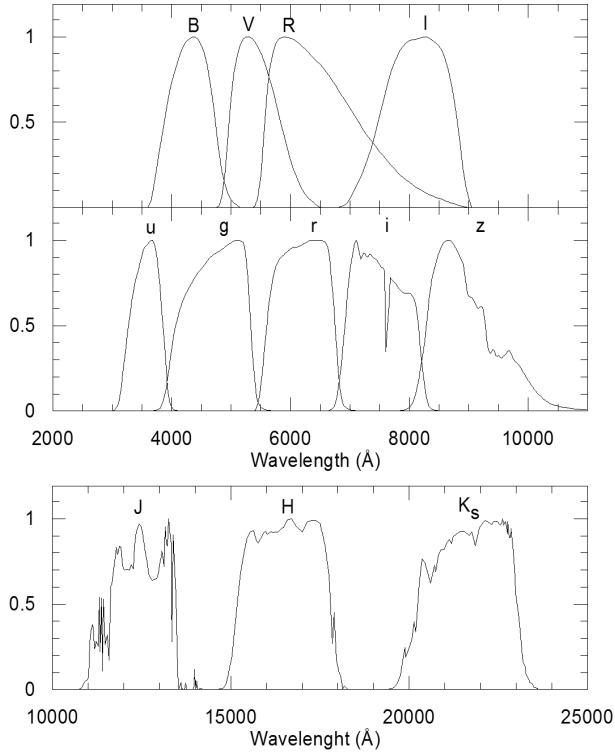


Fig. 1 Normalized passbands of the Johnson-Cousins' *BVRI* filters (upper panel), the *SDSS ugriz* filters (middle panel), and the *2MASS* filters (lower panel).

A number of transformations between $u'g'r'i'z'$, *ugriz* and $UBVR_cI_c$ exist. The $u'g'r'i'z'$ system is referred to the similar filter system used on the 0.5-m Photometric Calibration Telescope at SDSS. It should be noted that there are differences between the $u'g'r'i'z'$ and *ugriz* systems. These are discussed in Tucker et al. (2006), Davenport et al. (2007) and Smith et al. (2007). In this paper we are concerned with transformations to and from *ugriz* system of the 2.5-m. The first transformations derived between the SDSS $u'g'r'i'z'$ system and the Johnson-Cousins' photometric system were based on the observations in u' , g' , r' , i' and z' filters (Smith et al., 2002).

An improved set of transformations between the observations obtained in $u'g'r'$ filters at the Isaac Newton Telescope (INT) at La Palma, Spain, and the Landolt (1992) *UBV* standards is derived by Karaali et al. (2005). The INT filters were designed to reproduce the SDSS system. Karaali et al. (2005) presented for the first time transformation equations depending on two colors.

Rodgers et al. (2006) considered two-color or quadratic forms in their transformation equations. Jordi et al. (2006) used SDSS DR4 and *BVRI* photometry taken from different sources and derived population (and metallicity) dependent transformation equations between SDSS and *UBVRI* systems. A recent work is by Chonis & Gaskell (2008) who used transformations from SDSS *ugriz* to *UBVRI* not depending on luminosity class or metallicity to determine CCD

zero-points. Finally, we refer to our most recent paper where transformations between SDSS (and 2MASS) and *BVRI* photometric systems for dwarfs are given (Bilir et al., 2008).

The first transformations between 2MASS and other photometric systems are those of Walkowicz et al. (2004) and West et al. (2005) who determined the level of magnetic activity in M and L dwarfs. The aim of Davenport et al. (2007) in deriving equations between 2MASS and other photometric systems was to estimate the absolute magnitudes of cool stars. Covey et al. (2008) considered the *ugrizJHK_s* stellar locus and showed how it can be used to identify objects with unusual colors. A recent study by Straizys & Lazauskaite (2009) provided calibrations which can be used to obtain the color indices of 2MASS stars with known spectral types and luminosity classes. Straizys & Lazauskaite (2009) used the loci of giant stars with spectral types later than G5 to obtain their calibrations.

To extend the results of Bilir et al. (2008) to the giants domain is of great use, as it allows to derive absolute magnitudes and to produce distance determinations at relatively short distances where SDSS sources will be saturated. For example, red clump giants are now considered as well-known standard candles, as they show a very narrow luminosity function that constitute a compact and well-defined clump in a Hertzsprung-Russell diagram, particularly in the NIR. The absolute magnitude (M_K) and intrinsic colors, $(J - K_s)_0$, of the red clump giants are well established with very small metallicity dependences (see Cabrera-Lavers et al., 2008, and references therein), hence distances to these sources can be derived with confidence by means of a very small number of assumptions (López-Corredoira et al., 2002). This well known set of NIR properties of the red clump population have not been sufficiently studied in the optical, where a lot of SDSS data is waiting to be exploited. In order to do this, a proper set of optical/NIR photometric transformations are needed and these are presented here.

In Section 2 we present the sources of our star sample and the criteria applied to the chosen stars. The transformation equations are given in Section 3. Finally, in Section 4, we discuss our results.

2 Data

The first and main source of our data was Cayrel de Strobel et al.'s (2001) spectroscopic catalogue. This catalogue contains a large number of stars with different population types and metallicities. We chose 661 stars with $2 < \log g \leq 3$ and obtained the original sample of late-type giants. The second source for our work is the 2MASS All-Sky Catalogue of Point Sources (Cutri et al., 2003). We matched the Cayrel de Strobel et al.'s (2001) spectroscopic catalogue with the Cutri et al.'s (2003) 2MASS photometric catalogue and obtained the NIR magnitudes for 661 stars. The NIR magnitudes of 661 stars are not as precise as their optical magnitudes. To select more sensitive NIR magnitudes of sample stars, we used the magnitude flags, labeled "AAA",

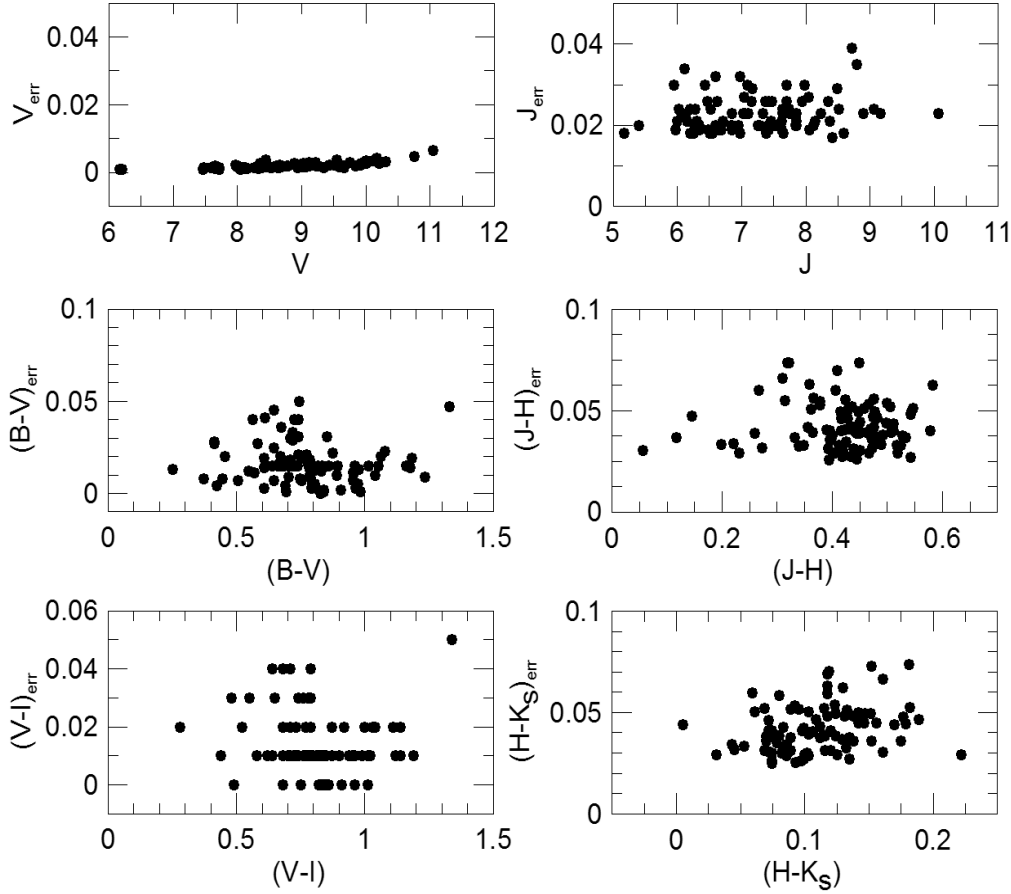


Fig. 2 The error distributions for Johnson-Cousins' BVI and 2MASS JHK_s (the errors for SDSS $griz$ magnitudes are discussed in the text).

which means the signal noise ratio is $SNR \geq 10$, i.e. they have the highest quality measurements.

After applying this selection criterion based on the quality of the data, the total number of stars in 2MASS photometric system was reduced to 91. The photometric and spectroscopic data of 91 stars is given in Table 1.

The BVI magnitudes were taken from the newly reduced Hipparcos' (van Leeuwen, 2007) catalogue. The same catalogue also offers trigonometric parallaxes which provides accurate distance determination. Finally, the g , r and i magnitudes were taken from the Ofek's (2008) catalogue. Ofek (2008) calculated the synthetic $griz$ magnitudes of bright Tycho stars, where SDSS magnitudes are actually saturated. Out of 91 stars only 82 had g , r and i magnitudes, due to the shallowness of 2MASS and deepness of the SDSS photometries. Thus, transformation equations between BVI and 2MASS is carried out for a sample of 91 stars, whereas the ones between SDSS and 2MASS is limited with 82 stars.

The errors for the colors and magnitudes for BVI and 2MASS photometries are given in Fig. 2. For SDSS magnitudes, Ofek (2008) states that the typical errors for a single star are 0.12, 0.12, 0.10 and 0.08 mag for g , r , i and z bands,

respectively, but they reduce to about 0.04, 0.03, 0.02 and 0.02 mag for a sample of about 10 stars.

The $E(B - V)$ color excesses of stars have been evaluated in two steps. First, we used the maps of Schlegel et al. (1998) and evaluated a $E_\infty(B - V)$ color excess for each star. We then reduced them using the following procedure (Bahcall & Soneira, 1980):

$$A_d(b) = A_\infty(b) \left[1 - \exp\left(\frac{-|d \sin(b)|}{H}\right) \right]. \quad (1)$$

Here, b and d are the galactic latitude and distance of the star, respectively. H is the scaleheight for the interstellar dust which is adopted as 125 pc (Marshall et al., 2006) and $A_\infty(b)$ and $A_d(b)$ are the total absorptions for the model and for the distance to the star, respectively. $A_\infty(b)$ can be evaluated by means of the following equation:

$$A_\infty(b) = 3.1E_\infty(B - V). \quad (2)$$

$E_\infty(B - V)$ is the color excess for the model taken from the NASA Extragalactic Database². Then, $E_d(B - V)$, i.e. the color excess for the corresponding star at the distance d , can be evaluated by Eq. (3) adopted for distance d ,

$$E_d(B - V) = A_d(b) / 3.1. \quad (3)$$

² <http://nedwww.ipac.caltech.edu/forms/calculator.html>

Table 1 Johnson-Cousins, SDSS and 2MASS magnitudes, coordinates and parallax of the sample stars (91 total stars). The columns give: (1) ID, (2) Hipparcos number, (3)-(5) surface gravity, metal abundance and their references (6) parallax, (7) relative parallax error, (8) distance (9) $E_d(B - V)$ reduced color excess, (10) V apparent magnitude, (11) and (12) $B - V$ and $V - I$ color indices, (13) g apparent magnitude, (14) and (15) $g - r$, $r - i$ color indices, (16) J apparent magnitude, (17) and (18) $J - H$ and $H - K_s$ color indices.

ID	Hip	$\log g$	$[M/H]$	Ref.	π	σ_π/π	d	$E_d(B - V)$	V	$B - V$	$V - I$	g	$g - r$	$r - i$	J	$J - H$	$H - K_s$
		(dex)			(mas)	(%)	(pc)	(mag)	(mag)	(mag)	(mag)	(mag)	(mag)	(mag)	(mag)	(mag)	(mag)
1	434	2.80	-1.39	1	2.58 ± 1.10	0.43	388	0.016	9.040 ± 0.002	0.692 ± 0.001	0.75 ± 0.01	9.330	0.480	0.150	7.704 ± 0.030	0.356 ± 0.042	0.099 ± 0.042
2	447	2.50	-0.45	2	2.99 ± 1.16	0.39	334	0.074	8.260 ± 0.002	1.052 ± 0.015	1.11 ± 0.02	8.790	0.730	0.270	6.540 ± 0.019	0.434 ± 0.028	0.074 ± 0.026
3	484	2.60	-1.19	3	0.37 ± 1.33	3.59	540*	0.021	9.660 ± 0.002	0.787 ± 0.016	0.82 ± 0.01	10.040	0.660	0.180	8.057 ± 0.019	0.445 ± 0.039	0.099 ± 0.041
4	999	3.00	-0.40	4	24.38 ± 0.95	0.04	41	0.011	8.440 ± 0.004	0.739 ± 0.015	0.79 ± 0.01	8.810	0.670	0.250	6.847 ± 0.023	0.467 ± 0.029	0.135 ± 0.027
5	1298	2.60	-1.17	1	1.06 ± 1.67	1.58	520*	0.020	9.580 ± 0.002	0.710 ± 0.030	0.76 ± 0.03	9.850	0.480	0.150	8.147 ± 0.021	0.361 ± 0.051	0.103 ± 0.051
6	2023	2.50	-0.11	5	7.29 ± 0.76	0.10	137	0.021	8.000 ± 0.002	0.253 ± 0.013	0.28 ± 0.02	8.160	0.120	0.000	7.415 ± 0.020	0.056 ± 0.030	0.031 ± 0.029
7	2413	2.50	-2.00	6	3.15 ± 0.78	0.25	317	0.086	7.720 ± 0.001	0.747 ± 0.008	0.79 ± 0.01	—	—	—	6.026 ± 0.024	0.423 ± 0.041	0.129 ± 0.037
8	2463	2.25	-2.10	7	0.88 ± 0.81	0.92	313*	0.019	8.480 ± 0.002	0.713 ± 0.015	0.77 ± 0.01	8.800	0.660	0.260	6.853 ± 0.020	0.462 ± 0.039	0.135 ± 0.038
9	2727	2.60	-1.04	3	3.47 ± 1.24	0.36	288	0.018	9.750 ± 0.003	0.735 ± 0.015	0.78 ± 0.01	10.080	0.480	0.150	8.376 ± 0.021	0.365 ± 0.039	0.106 ± 0.041
10	3554	3.00	-2.30	7	5.01 ± 1.32	0.26	200	0.029	9.020 ± 0.003	0.745 ± 0.050	0.79 ± 0.04	9.360	0.640	0.210	7.424 ± 0.026	0.449 ± 0.074	0.152 ± 0.073
11	4930	2.80	-0.25	8	2.59 ± 0.94	0.36	386	0.017	7.990 ± 0.002	0.983 ± 0.001	0.96 ± 0.01	8.530	0.780	0.260	6.203 ± 0.018	0.528 ± 0.038	0.116 ± 0.039
12	4960	2.53	-0.99	9	3.18 ± 0.93	0.29	314	0.027	8.600 ± 0.002	0.741 ± 0.031	0.79 ± 0.02	9.050	0.640	0.210	7.088 ± 0.030	0.442 ± 0.040	0.071 ± 0.031
13	5104	2.30	-0.93	10	3.19 ± 0.79	0.25	313	0.023	7.650 ± 0.002	0.785 ± 0.010	0.82 ± 0.01	8.090	0.640	0.210	6.149 ± 0.021	0.473 ± 0.032	0.089 ± 0.031
14	5445	2.50	-1.56	6	7.16 ± 0.84	0.12	140	0.021	7.720 ± 0.002	0.701 ± 0.009	0.76 ± 0.01	8.090	0.630	0.210	6.197 ± 0.024	0.438 ± 0.031	0.097 ± 0.026
15	5455	2.79	-0.83	9	7.23 ± 0.86	0.12	138	0.014	9.020 ± 0.002	0.803 ± 0.004	0.83 ± 0.01	9.440	0.660	0.180	7.459 ± 0.021	0.466 ± 0.053	0.092 ± 0.053
16	6894	2.30	-1.57	9	2.55 ± 1.04	0.41	392	0.010	8.930 ± 0.002	0.820 ± 0.014	0.84 ± 0.01	9.320	0.660	0.250	7.289 ± 0.020	0.558 ± 0.051	0.124 ± 0.050
17	12028	2.10	-0.21	11	4.12 ± 1.17	0.28	243	0.021	8.150 ± 0.001	1.235 ± 0.009	1.19 ± 0.01	8.850	0.950	0.330	6.062 ± 0.023	0.418 ± 0.029	0.222 ± 0.029
18	12353	3.00	-2.23	12	2.33 ± 1.20	0.52	664*	0.027	10.110 ± 0.004	0.782 ± 0.014	0.82 ± 0.01	10.420	0.600	0.220	5.595 ± 0.018	0.416 ± 0.040	0.080 ± 0.058
19	14747	3.00	-1.03	7	2.60 ± 0.74	0.28	385	0.018	8.900 ± 0.002	0.840 ± 0.002	0.86 ± 0.01	9.370	0.670	0.250	7.332 ± 0.023	0.482 ± 0.037	0.070 ± 0.036
20	16214	2.11	-1.75	13	4.03 ± 1.00	0.25	248	0.103	8.700 ± 0.002	0.786 ± 0.018	0.82 ± 0.01	9.110	0.670	0.220	6.975 ± 0.018	0.428 ± 0.050	0.133 ± 0.051
21	17001	2.60	-2.30	14	3.93 ± 1.53	0.39	254	0.015	9.920 ± 0.002	0.647 ± 0.045	0.71 ± 0.04	—	—	—	8.497 ± 0.029	0.400 ± 0.038	0.138 ± 0.036
22	18742	2.61	-2.31	9	2.55 ± 0.70	0.27	392	0.066	8.780 ± 0.002	0.709 ± 0.018	0.76 ± 0.01	9.140	0.630	0.210	7.172 ± 0.029	0.477 ± 0.049	0.061 ± 0.051
23	21473	2.20	-0.69	10	1.23 ± 0.65	0.53	449*	0.009	9.260 ± 0.002	0.907 ± 0.002	0.91 ± 0.01	9.740	0.720	0.260	7.588 ± 0.020	0.480 ± 0.047	0.151 ± 0.049
24	23799	2.20	0.19	15	4.20 ± 0.76	0.18	238	0.036	6.200 ± 0.001	0.444 ± 0.008	0.55 ± 0.03	6.420	0.360	0.100	5.167 ± 0.018	0.145 ± 0.048	0.118 ± 0.048
25	26040	3.00	-1.76	7	2.99 ± 0.86	0.29	334	0.024	9.430 ± 0.002	0.740 ± 0.021	0.79 ± 0.01	9.810	0.640	0.210	7.856 ± 0.023	0.415 ± 0.050	0.142 ± 0.050
26	28887	3.00	-1.64	12	2.25 ± 1.92	0.85	728*	0.174	10.31 ± 0.003	0.676 ± 0.036	0.74 ± 0.03	10.590	0.480	0.150	8.891 ± 0.023	0.359 ± 0.063	0.118 ± 0.063
27	29759	2.90	-2.31	16	6.46 ± 1.31	0.20	155	0.054	8.920 ± 0.002	0.611 ± 0.041	0.68 ± 0.04	9.240	0.480	0.160	7.532 ± 0.020	0.377 ± 0.053	0.069 ± 0.052
28	29992	2.20	-1.61	17	5.57 ± 0.84	0.15	180	0.065	8.050 ± 0.001	0.829 ± 0.012	0.85 ± 0.01	8.460	0.670	0.230	6.340 ± 0.020	0.534 ± 0.037	0.103 ± 0.039
29	30668	3.00	-1.58	18	6.72 ± 0.70	0.10	149	0.063	8.000 ± 0.002	0.703 ± 0.015	0.76 ± 0.01	8.360	0.610	0.220	6.591 ± 0.020	0.321 ± 0.074	0.181 ± 0.074
30	34795	2.80	-1.55	19	1.94 ± 0.91	0.47	515	0.101	8.370 ± 0.002	0.955 ± 0.007	1.00 ± 0.02	8.890	0.840	0.320	6.590 ± 0.032	0.547 ± 0.051	0.112 ± 0.043
31	37335	3.00	-1.02	20	5.17 ± 1.32	0.26	193	0.022	9.230 ± 0.002	0.820 ± 0.002	0.84 ± 0.01	9.640	0.660	0.260	7.621 ± 0.021	0.437 ± 0.042	0.146 ± 0.045
32	37339	3.00	0.25	15	9.84 ± 0.47	0.05	102	0.016	6.160 ± 0.001	0.374 ± 0.008	0.44 ± 0.01	6.340	0.240	0.010	5.404 ± 0.020	0.117 ± 0.037	0.071 ± 0.037
33	40068	3.00	-2.05	21	4.97 ± 1.07	0.22	201	0.015	10.010 ± 0.003	0.564 ± 0.040	0.64 ± 0.04	—	—	—	8.711 ± 0.039	0.378 ± 0.054	0.072 ± 0.046
34	44636	2.50	0.13	22	0.84 ± 0.99	1.18	327*	0.077	8.570 ± 0.002	1.160 ± 0.015	1.12 ± 0.01	9.190	0.950	0.330	6.472 ± 0.026	0.499 ± 0.054	0.182 ± 0.052
35	44716	3.00	-1.02	12	1.84 ± 1.23	0.67	217*	0.027	7.680 ± 0.001	0.796 ± 0.014	0.83 ± 0.01	8.080	0.650	0.190	6.105 ± 0.034	0.511 ± 0.043	0.043 ± 0.034
36	45845	2.30	-0.89	10	3.13 ± 0.60	0.19	319	0.061	8.410 ± 0.002	0.975 ± 0.013	1.02 ± 0.01	8.860	0.790	0.270	6.516 ± 0.024	0.542 ± 0.048	0.142 ± 0.045
37	47139	2.20	-1.52	6	0.96 ± 0.77	0.80	292*	0.034	8.330 ± 0.001	1.015 ± 0.015	0.99 ± 0.01	8.940	0.980	0.370	6.307 ± 0.021	0.578 ± 0.040	0.120 ± 0.041
38	47599	2.40	-1.40	23	0.53 ± 0.92	1.74	466*	0.010	9.340 ± 0.002	0.644 ± 0.025	0.71 ± 0.02	9.570	0.480	0.150	7.860 ± 0.021	0.393 ± 0.031	0.100 ± 0.029
39	48444	2.20	-2.45	6	0.90 ± 1.50	1.67	611*	0.010	9.930 ± 0.003	0.835 ± 0.015	0.85 ± 0.01	—	—	—	8.355 ± 0.026	0.424 ± 0.055	0.115 ± 0.052
40	48979	2.10	-0.97	10	0.96 ± 1.26	1.31	540*	0.048	9.660 ± 0.002	0.826 ± 0.001	0.85 ± 0.01	10.090	0.660	0.250	8.050 ± 0.027	0.470 ± 0.041	0.089 ± 0.037
41	49371	2.58	-2.02	24	3.62 ± 1.22	0.34	276	0.005	8.970 ± 0.002	0.719 ± 0.033	0.77 ± 0.02	—	—	—	7.471 ± 0.026	0.425 ± 0.035	0.103 ± 0.029
42	49616	3.00	-2.23	12	8.75 ± 0.62	0.07	114	0.054	8.660 ± 0.002	0.663 ± 0.016	0.72 ± 0.01	9.020	0.640	0.210	7.032 ± 0.023	0.428 ± 0.046	0.177 ± 0.048
43	50601	2.80	0.10	19	5.12 ± 0.77	0.15	195	0.028	7.480 ± 0.001	0.958 ± 0.011	0.95 ± 0.01	8.020	0.820	0.270	5.941 ± 0.030	0.476 ± 0.056	0.147 ± 0.050
44	50994	2.10	0.19	11	1.72 ± 1.04	0.60	515*	0.107	9.560 ± 0.002	1.330 ± 0.047	1.34 ± 0.05	10.140	0.950	0.330	7.375 ± 0.026	0.544 ± 0.049	0.189 ± 0.047
45	53561	2.60	-0.02	22	2.58 ± 0.79	0.31	388	0.043	8.450 ± 0.002	0.960 ± 0.015	0.95 ± 0.01	8.900	0.730	0.270	6.712 ± 0.021	0.474 ± 0.047	0.131 ± 0.048
46	53810	2.10	0.01	11	5.08 ± 0.84	0.17	197	0.036	8.350 ± 0.001	1.176 ± 0.014	1.14 ± 0.01	8.950	0.870	0.300	6.431 ± 0.030	0.583 ± 0.063	0.130 ± 0.062
47	56074	2.20	-1.12	10	2.87 ± 0.91	0.32	348	0.102	8.650 ± 0.001	0.955 ± 0.011	0.94 ± 0.01	9.170	0.780	0.260	6.837 ± 0.020	0.506 ± 0.039	0.145 ± 0.047
48	56551	2.20	-0.59	11	3.45 ± 0.99	0.29	290	0.032	8.770 ± 0.002	1.077 ± 0.023	1.04 ± 0.02	—	—	—	7.048 ± 0.023	0.448 ± 0.050	0.447 ± 0.047
49	57982	2.60	-1.04	10	1.10 ± 1.19	1.08	520*	0.071	9.580 ± 0.002	0.791 ± 0.007	0.82 ± 0.01	9.980	0.660	0.260	7.945 ± 0.026	0.447 ± 0.043	0.124 ± 0.038
50	57983	2.50	-2.25	1	2.02 ± 1.10	0.54	522*	0.021	9.590 ± 0.002	0.725 ± 0.040	0.78 ± 0.03	9.960	0.610	0.210	8.126 ± 0.020	0.409 ± 0.070	0.119 ± 0.070

ID	Hip	log <i>g</i>	[<i>M</i> / <i>H</i>]	Ref.	π	σ_{π}/π	<i>d</i>	$E_d(B-V)$	<i>V</i>	<i>B</i> - <i>V</i>	<i>V</i> - <i>I</i>	<i>g</i>	<i>g</i> - <i>r</i>	<i>r</i> - <i>i</i>	<i>J</i>	<i>J</i> - <i>H</i>	<i>H</i> - <i>K_s</i>
			(dex)		(mas)		(pc)	(mag)	(mag)	(mag)	(mag)	(mag)	(mag)	(mag)	(mag)	(mag)	(mag)
51	58357	2.50	-0.82	25	6.85 ± 0.99	0.14	146	0.019	8.350 ± 0.001	0.860 ± 0.015	0.87 ± 0.01	8.830	0.680	0.220	6.681 ± 0.019	0.420 ± 0.031	0.102 ± 0.030
52	59109	3.00	-2.62	21	4.87 ± 1.51	0.31	205	0.036	10.000 ± 0.003	0.413 ± 0.027	0.48 ± 0.03	10.130	0.250	0.050	9.064 ± 0.024	0.266 ± 0.060	0.059 ± 0.060
53	59239	2.40	-1.20	23	2.88 ± 0.74	0.26	347	0.020	8.610 ± 0.002	0.660 ± 0.015	0.72 ± 0.01	—	—	—	7.152 ± 0.026	0.396 ± 0.035	0.082 ± 0.030
54	59334	2.50	-0.51	26	4.91 ± 0.92	0.19	204	0.033	8.370 ± 0.002	0.974 ± 0.005	0.96 ± 0.01	8.850	0.780	0.270	6.506 ± 0.018	0.543 ± 0.027	0.116 ± 0.031
55	60719	2.30	-2.30	14	5.73 ± 0.67	0.12	175	0.013	8.030 ± 0.001	0.607 ± 0.014	0.68 ± 0.01	8.340	0.480	0.150	6.623 ± 0.026	0.390 ± 0.040	0.080 ± 0.039
56	61175	2.80	-0.21	19	3.65 ± 0.81	0.22	274	0.042	8.090 ± 0.001	1.040 ± 0.010	1.01 ± 0.01	8.620	0.810	0.290	6.278 ± 0.024	0.505 ± 0.052	0.138 ± 0.048
57	62235	2.54	-1.44	9	0.52 ± 1.08	2.08	425*	0.016	9.140 ± 0.002	0.672 ± 0.015	0.73 ± 0.01	9.460	0.510	0.140	7.852 ± 0.020	0.309 ± 0.066	0.161 ± 0.066
58	62747	2.87	-1.25	27	4.33 ± 0.86	0.20	231	0.040	7.970 ± 0.002	0.800 ± 0.012	0.83 ± 0.01	8.390	0.660	0.260	6.347 ± 0.019	0.449 ± 0.039	0.112 ± 0.038
59	63955	2.20	-0.26	11	1.54 ± 0.82	0.53	316*	0.071	8.500 ± 0.002	1.183 ± 0.019	1.14 ± 0.02	9.120	0.980	0.350	6.631 ± 0.019	0.471 ± 0.036	0.175 ± 0.036
60	64115	2.69	-0.35	28	4.71 ± 1.03	0.22	212	0.032	8.350 ± 0.003	0.963 ± 0.003	1.01 ± 0.01	8.880	0.780	0.270	6.541 ± 0.018	0.498 ± 0.044	0.156 ± 0.045
61	65819	2.70	-0.86	10	4.38 ± 1.06	0.24	228	0.025	9.010 ± 0.002	0.839 ± 0.001	0.86 ± 0.01	9.510	0.680	0.220	7.386 ± 0.018	0.512 ± 0.040	0.072 ± 0.041
62	68246	2.94	-0.66	29	8.62 ± 0.91	0.11	116	0.050	8.610 ± 0.002	0.424 ± 0.004	0.49 ± 0.01	—	—	—	7.695 ± 0.026	0.259 ± 0.039	0.005 ± 0.044
63	69089	2.60	0.04	30	-0.43 ± 0.85	-1.98	344*	0.015	8.680 ± 0.002	1.062 ± 0.020	1.03 ± 0.02	9.180	0.730	0.270	6.952 ± 0.020	0.412 ± 0.033	0.161 ± 0.031
64	70519	2.16	-1.78	27	3.82 ± 0.77	0.20	262	0.054	7.660 ± 0.001	0.791 ± 0.003	0.82 ± 0.01	8.080	0.680	0.220	5.975 ± 0.019	0.517 ± 0.033	0.120 ± 0.031
65	70647	3.00	-2.20	7	0.89 ± 1.23	1.38	419*	0.085	9.110 ± 0.002	0.774 ± 0.021	0.81 ± 0.01	9.530	0.850	0.310	7.258 ± 0.020	0.481 ± 0.047	0.109 ± 0.047
66	71087	2.20	-1.58	1	2.34 ± 1.39	0.59	586*	0.020	9.840 ± 0.002	0.818 ± 0.015	0.84 ± 0.01	10.110	0.610	0.220	8.241 ± 0.023	0.404 ± 0.029	0.093 ± 0.025
67	71458	2.50	-2.50	31	6.09 ± 1.08	0.18	164	0.046	8.020 ± 0.002	0.640 ± 0.015	0.70 ± 0.01	8.370	0.610	0.220	6.568 ± 0.019	0.417 ± 0.028	0.086 ± 0.029
68	71761	3.00	-0.92	7	5.42 ± 1.49	0.27	185	0.053	9.220 ± 0.003	0.606 ± 0.019	0.68 ± 0.02	9.510	0.460	0.130	7.981 ± 0.030	0.314 ± 0.055	0.095 ± 0.052
69	72561	3.00	-1.61	32	5.00 ± 2.23	0.45	200	0.031	11.050 ± 0.007	0.413 ± 0.028	0.48 ± 0.03	11.110	0.270	0.050	10.062 ± 0.023	0.220 ± 0.034	0.053 ± 0.033
70	78378	2.17	-0.77	9	6.35 ± 0.78	0.12	157	0.121	8.020 ± 0.002	0.972 ± 0.013	0.96 ± 0.01	8.520	0.780	0.270	6.139 ± 0.023	0.474 ± 0.039	0.152 ± 0.036
71	80822	3.00	-0.90	23	3.50 ± 1.08	0.31	286	0.042	9.060 ± 0.002	0.672 ± 0.020	0.73 ± 0.02	9.420	0.560	0.190	7.619 ± 0.019	0.348 ± 0.033	0.086 ± 0.034
72	82315	2.81	-0.63	9	0.40 ± 1.22	3.05	377*	0.123	8.880 ± 0.003	0.852 ± 0.031	0.87 ± 0.02	9.280	0.730	0.270	7.101 ± 0.023	0.416 ± 0.046	0.170 ± 0.044
73	85855	2.92	-2.35	29	3.62 ± 1.05	0.29	276	0.041	8.940 ± 0.002	0.607 ± 0.003	0.68 ± 0.01	9.240	0.610	0.220	7.420 ± 0.019	0.394 ± 0.025	0.074 ± 0.025
74	88977	3.00	-1.00	33	4.56 ± 0.84	0.18	219	0.206	8.120 ± 0.001	0.875 ± 0.022	0.92 ± 0.02	8.680	0.980	0.380	5.998 ± 0.021	0.475 ± 0.042	0.179 ± 0.044
75	90659	3.00	0.67	34	8.95 ± 0.71	0.08	112	0.023	8.130 ± 0.001	0.803 ± 0.005	0.83 ± 0.01	8.530	0.650	0.220	6.478 ± 0.019	0.451 ± 0.031	0.074 ± 0.030
76	96248	2.64	-1.85	9	4.97 ± 0.71	0.14	201	0.052	7.590 ± 0.001	0.548 ± 0.012	0.62 ± 0.01	7.850	0.500	0.150	6.252 ± 0.018	0.339 ± 0.032	0.083 ± 0.031
77	97747	3.00	-1.40	35	6.29 ± 2.02	0.32	159	0.036	10.760 ± 0.005	0.740 ± 0.040	0.79 ± 0.03	11.130	0.650	0.190	9.161 ± 0.023	0.430 ± 0.041	0.074 ± 0.041
78	98883	3.00	-1.00	7	5.46 ± 1.32	0.24	183	0.051	9.510 ± 0.002	0.507 ± 0.007	0.58 ± 0.01	9.800	0.390	0.150	8.416 ± 0.017	0.273 ± 0.032	0.069 ± 0.031
79	98974	2.25	-1.79	7	4.78 ± 0.98	0.21	209	0.129	8.530 ± 0.001	0.753 ± 0.019	0.80 ± 0.01	8.930	0.640	0.210	6.970 ± 0.032	0.451 ± 0.045	0.078 ± 0.035
80	103337	2.30	-2.26	25	1.81 ± 1.59	0.88	695*	0.033	10.210 ± 0.003	0.893 ± 0.015	0.90 ± 0.01	10.640	0.680	0.220	8.511 ± 0.024	0.489 ± 0.033	0.083 ± 0.043
81	104191	2.50	-3.16	36	2.54 ± 1.15	0.45	394	0.025	9.090 ± 0.002	0.582 ± 0.027	0.65 ± 0.03	—	—	—	7.648 ± 0.018	0.396 ± 0.040	0.098 ± 0.041
82	105993	2.30	-1.57	6	3.23 ± 1.71	0.53	682*	0.054	10.170 ± 0.004	0.719 ± 0.015	0.77 ± 0.01	10.430	0.510	0.140	8.800 ± 0.035	0.319 ± 0.074	0.118 ± 0.069
83	109390	2.20	-1.34	21	4.18 ± 1.30	0.31	239	0.031	9.550 ± 0.004	0.892 ± 0.010	0.90 ± 0.01	10.010	0.780	0.260	7.839 ± 0.020	0.524 ± 0.033	0.132 ± 0.033
84	109501	2.93	-0.81	24	6.48 ± 1.84	0.28	154	0.033	8.630 ± 0.001	0.454 ± 0.020	0.52 ± 0.02	8.970	0.360	0.100	7.642 ± 0.023	0.198 ± 0.033	0.045 ± 0.032
85	110271	2.20	-1.03	10	0.76 ± 1.47	1.93	421*	0.018	9.120 ± 0.003	0.753 ± 0.007	0.80 ± 0.01	9.530	0.640	0.210	7.642 ± 0.024	0.436 ± 0.052	0.089 ± 0.052
86	111228	2.85	-1.40	9	4.04 ± 1.01	0.25	248	0.011	8.520 ± 0.001	0.685 ± 0.015	0.74 ± 0.01	8.870	0.610	0.210	7.041 ± 0.027	0.492 ± 0.038	0.070 ± 0.038
87	112457	2.02	-1.35	9	1.23 ± 0.90	0.73	310*	0.013	8.460 ± 0.002	0.776 ± 0.017	0.81 ± 0.01	8.880	0.660	0.250	6.850 ± 0.019	0.445 ± 0.026	0.125 ± 0.029
88	112821	2.80	-0.55	37	8.72 ± 0.59	0.07	115	0.029	7.460 ± 0.001	0.647 ± 0.007	0.71 ± 0.01	7.800	0.470	0.170	6.265 ± 0.020	0.231 ± 0.029	0.099 ± 0.027
89	114502	2.40	-1.86	1	3.21 ± 1.09	0.34	312	0.032	8.940 ± 0.002	0.718 ± 0.029	0.77 ± 0.02	9.270	0.630	0.210	7.397 ± 0.019	0.406 ± 0.060	0.118 ± 0.059
90	116285	2.49	-1.14	9	0.76 ± 1.28	1.68	433*	0.009	9.180 ± 0.002	0.689 ± 0.004	0.75 ± 0.01	9.500	0.610	0.220	7.736 ± 0.024	0.366 ± 0.056	0.123 ± 0.054
91	117168	2.64	-1.51	9	2.48 ± 0.74	0.30	403	0.020	9.020 ± 0.002	0.571 ± 0.011	0.64 ± 0.01	9.310	0.450	0.160	7.747 ± 0.023	0.332 ± 0.037	0.077 ± 0.039

(*) The derived distance using the method explained in this paper

- (1) Pilachowski et al. (1996), (2) Smith & Lambert (1986), (3) Burris et al. (2000), (4) Spite et al. (1994), (5) Kovacs (1983), (6) Gilroy et al. (1988), (7) Gratton (1983), (8) Barbuy & Erdelyi-Mendes (1989), (9) Gratton et al. (2000), (10) Ryan & Lambert (1995), (11) Dominy (1984), (12) Ryan & Deliyannis (1998), (13) Gratton (1989), (14) Luck & Bond (1985), (15) Luck & Wepfer (1995), (16) Fulbright & Kraft (1999), (17) Kraft et al. (1992), (18) Tomkin & Lambert (1999), (19) Luck & Bond (1991), (20) Peterson (1981), (21) Fulbright (2000), (22) Drake & Lambert (1994), (23) Gratton & Ortolani (1984), (24) Tomkin et al. (1992), (25) Cavallo et al. (1997), (26) Shetrone (1996), (27) Gratton & Sneden (1991), (28) Clementini et al. (1999), (29) Axer et al. (1994), (30) Luck & Challener (1995), (31) Spite & Spite (1980), (32) Spite et al. (1993), (33) Leep & Wallerstein (1981), (34) Mishenina et al. (1995), (35) Carney et al. (1997), (36) Ryan et al. (1991), (37) Krishnaswamy & Sneden (1985).

We have omitted the indices ∞ and d from the color excess $E(B - V)$ in the equations. However, we use the terms model for the color excess of Schlegel et al. (1998) and “reduced” the color excess corresponding to distance d . The total absorption A_d used in this section and the classical total absorption A_V have the same meaning.

The distances of 65 stars whose relative parallax errors are small were evaluated by using their original parallaxes. However, for one star with negative trigonometric parallax and for 25 stars with relative parallax errors $\sigma_\pi/\pi > 0.5$ the following formula was used for this purpose:

$$V - M_V - A_d(b) = 5 \log d - 5. \quad (4)$$

The absolute magnitudes for this sub-sample of stars were adopted as $M_V = 1$. The distances derived using this method are denoted with a star superscript in Table 1. As the total absorptions for the model and distance to the star are different, the distance to a star in this category (a total of 26 stars), as well as its total absorption, $A_d(b)$, and color excess, $E_d(B - V)$, could be evaluated by iterating Eqs. (1)–(4).

We de-reddened the colors and magnitudes by using the $E_d(B - V)$ color index of the stars evaluated using the procedures explained above and the equations of Fan (1999); Fiorucci & Munari (2003); Yadav & Sagar (2004) for $V - I$ color, and for 2MASS and SDSS photometries, respectively. The related equations are given in the following:

$$\begin{aligned} V_0 &= V - 3.1E_d(B - V), \\ (B - V)_0 &= (B - V) - E_d(B - V), \\ (V - I)_0 &= (V - I) - 1.250E_d(B - V), \\ J_0 &= J - 0.887E_d(B - V), \\ (J - H)_0 &= (J - H) - 0.322E_d(B - V), \\ (H - K_s)_0 &= (H - K_s) - 0.183E_d(B - V), \\ g_0 &= g - 1.199E_d(B - V), \\ (g - r)_0 &= (g - r) - 0.341E_d(B - V), \\ (r - i)_0 &= (r - i) - 0.219E_d(B - V). \end{aligned} \quad (5)$$

The two color diagrams of the star sample for three photometric systems, i.e. BVI , gri and JHK_s , compared to the calibrations of Pickles (1998), Covey et al. (2008) and Straizys & Lazauskaite (2009) are given in Fig. 3, respectively. The valid color index intervals for the transformations for giants are as follows: $0.25 < (B - V)_0 < 1.35$, $0.25 < (V - I)_0 < 1.35$, $0.10 < (g - r)_0 < 0.95$, $0 < (r - i)_0 < 0.35$, $0.05 < (J - H)_0 < 0.60$, $0 < (H - K_s)_0 < 0.45$. The metallicity distribution of the sample covers all three populations, i.e. thin and thick disks, and halo (Fig. 4). The modes for the distributions of the whole sample (91 stars) and for the sample of stars (82 stars) which do not supply the relative parallax error condition ($\sigma_\pi/\pi < 0.5$) are -1.23 and -1.21 dex, respectively. The corresponding medians of these distributions are close to the modes (-1.18 and -1.12 dex) indicating two Gaussian distributions.

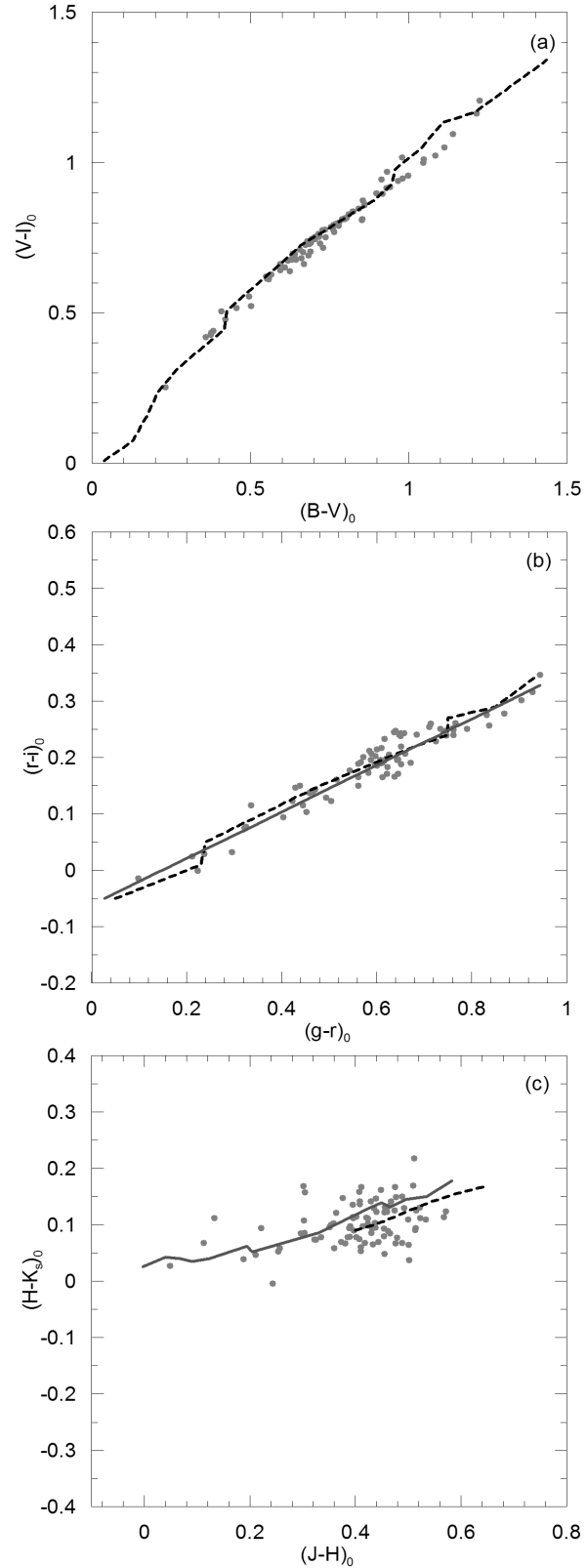


Fig. 3 Two-color diagrams of the sample stars. In all panels, the grey circles correspond to the positions of our sample stars. The dashed lines in panels (a), (b) and (c) are the calibrations of Pickles (1998), Covey et al. (2008), and Straizys & Lazauskaite (2009), respectively. (The continuous lines in panels (b) and (c) correspond to the two-color calibrations evaluated by the converted colors in Table 4. See section 4).

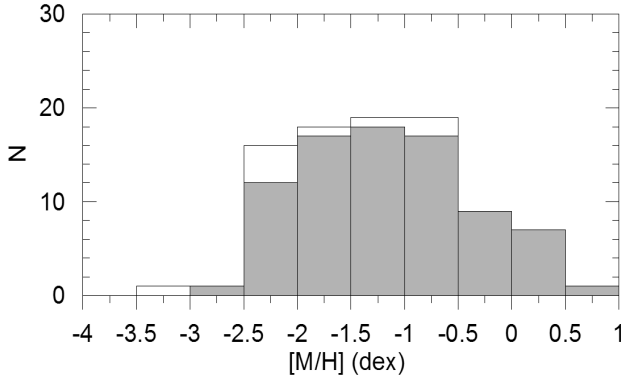


Fig. 4 Metallicity distributions for two samples: (1) for 91 late-type giant stars used in the transformations between BVI and JHK_s magnitudes (white area) and (2) for 82 giant stars used in the transformations between gri and JHK_s magnitudes (grey area).

3 Results

3.1 Transformations between 2MASS and Johnson–Cousins photometry

We used the following general equations and derived 12 sets of transformations between 2MASS and Johnson–Cousins BVI . Eqs. (6)–(11) transform 2MASS colors and magnitudes into BVI magnitudes, whereas Eqs. (12)–(17) are their inverse transformations. The transformations are either metallicity dependent (Eqs. (6)–(8) and (12)–(14)) or independent of metallicity (Eqs. (9)–(11) and (15)–(17)). In this work, we followed a procedure different than the one in Bilir et al. (2008), used for the dwarfs. Bilir et al. (2008) separated the sample of stars into metal-rich, intermediate metallicity and metal-poor sub-samples and obtained transformations for each sub-sample, whereas we adopted the metallicity as an additional term in Eqs. (6)–(8) and (12)–(14). This approach can be explained by the fact that stars change their positions in two color diagrams by shifting an amount proportional to their metallicities. The general equations are

$$(B-J)_0 = a_1(J-H)_0 + b_1(H-K_s)_0 + c_1[M/H] + d_1, \quad (6)$$

$$(V-J)_0 = a_2(J-H)_0 + b_2(H-K_s)_0 + c_2[M/H] + d_2, \quad (7)$$

$$(I-J)_0 = a_3(J-H)_0 + b_3(H-K_s)_0 + c_3[M/H] + d_3, \quad (8)$$

$$(B-J)_0 = a_4(J-H)_0 + b_4(H-K_s)_0 + d_4, \quad (9)$$

$$(V-J)_0 = a_5(J-H)_0 + b_5(H-K_s)_0 + d_5, \quad (10)$$

$$(I-J)_0 = a_6(J-H)_0 + b_6(H-K_s)_0 + d_6, \quad (11)$$

$$(V-J)_0 = e_1(B-V)_0 + f_1(V-I)_0 + g_1[M/H] + h_1, \quad (12)$$

$$(V-H)_0 = e_2(B-V)_0 + f_2(V-I)_0 + g_2[M/H] + h_2, \quad (13)$$

$$(V-K_s)_0 = e_3(B-V)_0 + f_3(V-I)_0 + g_3[M/H] + h_3, \quad (14)$$

$$(V-J)_0 = e_4(B-V)_0 + f_4(V-I)_0 + h_4, \quad (15)$$

$$(V-H)_0 = e_5(B-V)_0 + f_5(V-I)_0 + h_5, \quad (16)$$

$$(V-K_s)_0 = e_6(B-V)_0 + f_6(V-I)_0 + h_6. \quad (17)$$

The numerical values of the coefficients in Eqs. (6)–(17) are given in Table 2.

Table 1 Coefficients for the transformation Eqs. (6)–(17) in column matrix. The subscript $i = 1, 2$ and 3 or $i = 4, 5$ and 6 correspond to the same number that denotes the equations. R and s are the correlation coefficient and standard deviation for each category, respectively.

Equations dependent on metallicity, $i = 1, 2, 3$			
Coefficient	$(B-J)_0$	$(V-J)_0$	$(I-J)_0$
a_i	3.732 ± 0.163	2.328 ± 0.102	1.097 ± 0.089
b_i	2.125 ± 0.312	1.128 ± 0.195	0.306 ± 0.170
c_i	0.114 ± 0.019	0.033 ± 0.012	-0.031 ± 0.011
d_i	0.592 ± 0.071	0.435 ± 0.044	0.185 ± 0.038
R	0.950	0.945	0.832
s	0.142	0.089	0.077
Equations independent from metallicity, $i = 4, 5, 6$			
Coefficient	$(B-J)_0$	$(V-J)_0$	$(I-J)_0$
a_i	3.671 ± 0.191	2.310 ± 0.105	1.114 ± 0.092
b_i	2.518 ± 0.359	1.242 ± 0.198	0.198 ± 0.173
d_i	0.436 ± 0.077	0.390 ± 0.042	0.228 ± 0.037
R	0.929	0.940	0.812
s	0.167	0.092	0.080
Equations dependent on metallicity, $i = 1, 2, 3$			
Coefficient	$(V-J)_0$	$(V-H)_0$	$(V-K_s)_0$
e_i	1.080 ± 0.433	1.454 ± 0.590	1.791 ± 0.592
f_i	0.379 ± 0.495	0.504 ± 0.674	0.294 ± 0.676
g_i	-0.082 ± 0.015	-0.127 ± 0.020	-0.129 ± 0.020
h_i	0.279 ± 0.078	0.261 ± 0.106	0.276 ± 0.106
R	0.933	0.931	0.940
s	0.097	0.133	0.133
Equations independent from metallicity, $i = 4, 5, 6$			
Coefficient	$(V-J)_0$	$(V-H)_0$	$(V-K_s)_0$
e_i	0.397 ± 0.484	0.402 ± 0.684	0.716 ± 0.690
f_i	1.018 ± 0.560	1.488 ± 0.792	1.299 ± 0.799
h_i	0.396 ± 0.087	0.441 ± 0.123	0.460 ± 0.124
R	0.907	0.896	0.908
s	0.113	0.160	0.162

3.2 Transformations between 2MASS and SDSS

The transformations between 2MASS and SDSS, given in the following, have similar general equations:

$$(g-J)_0 = k_1(J-H)_0 + l_1(H-K_s)_0 + m_1[M/H] + n_1. \quad (18)$$

$$(r-J)_0 = k_2(J-H)_0 + l_2(H-K_s)_0 + m_2[M/H] + n_2. \quad (19)$$

$$(i-J)_0 = k_3(J-H)_0 + l_3(H-K_s)_0 + m_3[M/H] + n_3. \quad (20)$$

$$(g-J)_0 = k_4(J-H)_0 + l_4(H-K_s)_0 + n_4. \quad (21)$$

$$(r-J)_0 = k_5(J-H)_0 + l_5(H-K_s)_0 + n_5. \quad (22)$$

$$(i-J)_0 = k_6(J-H)_0 + l_6(H-K_s)_0 + n_6. \quad (23)$$

$$(g-J)_0 = o_1(g-r)_0 + p_1(r-i)_0 + r_1[M/H] + s_1. \quad (24)$$

$$(g-H)_0 = o_2(g-r)_0 + p_2(r-i)_0 + r_2[M/H] + s_2. \quad (25)$$

$$(g-K_s)_0 = o_3(g-r)_0 + p_3(r-i)_0 + r_3[M/H] + s_3. \quad (26)$$

$$(g-J)_0 = o_4(g-r)_0 + p_4(r-i)_0 + s_4. \quad (27)$$

$$(g-H)_0 = o_5(g-r)_0 + p_5(r-i)_0 + s_5. \quad (28)$$

$$(g-K_s)_0 = o_6(g-r)_0 + p_6(r-i)_0 + s_6. \quad (29)$$

One can see that, the equations which convert 2MASS colors and magnitudes into gri magnitudes and their inverse transformations are either metallicity dependent or independent of metallicity. The numerical values of the coefficients in Eqs. (18)–(29) are given in Table 3.

Table 2 Coefficients for the transformation Eqs. (18)–(29) in column matrix. The subscript $i = 1, 2$ and 3 or $i = 4, 5$ and 6 correspond to the same number that denotes the equations. R and s are the correlation coefficient and standard deviation for each category, respectively.

Equations dependent on metallicity, $i = 1, 2, 3$			
Coefficient	$(g - J)_0$	$(r - J)_0$	$(i - J)_0$
k_i	2.992 ± 0.127	1.743 ± 0.087	1.233 ± 0.083
l_i	2.478 ± 0.357	1.250 ± 0.245	0.727 ± 0.232
m_i	0.089 ± 0.016	0.054 ± 0.011	0.042 ± 0.010
n_i	0.461 ± 0.057	0.462 ± 0.039	0.524 ± 0.037
R	0.960	0.943	0.901
s	0.106	0.073	0.069
Equations independent from metallicity, $i = 4, 5, 6$			
	$(g - J)_0$	$(r - J)_0$	$(i - J)_0$
k_i	2.923 ± 0.148	1.701 ± 0.099	1.200 ± 0.090
l_i	3.031 ± 0.400	1.585 ± 0.266	0.991 ± 0.243
n_i	0.329 ± 0.061	0.383 ± 0.041	0.461 ± 0.037
R	0.943	0.925	0.879
s	0.124	0.083	0.075
Equations dependent on metallicity, $i = 1, 2, 3$			
	$(g - J)_0$	$(g - H)_0$	$(g - K_s)_0$
o_i	2.150 ± 0.199	2.767 ± 0.270	2.885 ± 0.267
p_i	0.194 ± 0.462	0.097 ± 0.627	0.130 ± 0.618
r_i	0.008 ± 0.012	-0.021 ± 0.017	-0.015 ± 0.016
s_i	0.531 ± 0.050	0.556 ± 0.068	0.590 ± 0.067
R	0.977	0.972	0.975
s	0.081	0.110	0.108
Equations independent from metallicity, $i = 4, 5, 6$			
	$(g - J)_0$	$(g - H)_0$	$(g - K_s)_0$
o_i	2.172 ± 0.196	2.706 ± 0.267	2.842 ± 0.262
p_i	0.160 ± 0.457	0.185 ± 0.626	0.192 ± 0.614
s_i	0.514 ± 0.043	0.600 ± 0.058	0.622 ± 0.057
R	0.976	0.972	0.975
s	0.081	0.110	0.108

3.3 Residuals

We compared the observed colors with those evaluated via Eqs. (6)–(29). The residuals are plotted versus observed $(B - V)_0$, $(J - H)_0$ or $(g - r)_0$ colors in Fig. 5. There are some small systematic deviations in the red and blue ends of the $(B - V)_0$ color. However, they are negligible when compared to the accuracy of the transformations. Actually, the mean of the residuals are smaller than a thousandth and the standard deviations are close to 0.1 mag for all colors (Table 4). The ranges of the residuals for different colors are not the same. The residuals are larger for colors over wider wavelength intervals but they are smaller for metal dependent transformations than the corresponding ones for metal independent transformations. One can confirm this argument by comparing the ranges of the residuals in Fig. 5 and the standard deviations in Table 4.

4 Discussion

We present color transformations for late-type giants from 2MASS photometric system into the Johnson–Cousins system

and furthermore into the SDSS system. Thus, this is the complement of the paper of Bilir et al. (2008) where transformations were carried out for dwarfs. We adopted the following steps in order to obtain accurate transformations: (1) the sample was selected by means of the star surface gravities, i.e. $2 < \log g \leq 3$, (2) the photometric data was de-reddened, (3) stars in the sample were selected according to their photometric data quality, (4) transformations were constructed as two-color dependent equations. Step (3) is especially important for 2MASS data because the inherent errors are larger relative to those in other photometries. Additionally, the transformations are given either as a function of metallicity or independent from metallicity. However, in the case of metallicity dependent equations the procedure is different than the one of Bilir et al.’s (2008). Instead of separating the star sample into different metallicity intervals, we added the metallicity as a term into the transformation equations.

The coefficients of the color terms in the same transformation equation are significant (see Tables 2 and 3) which indicate that the transformations are two-color dependent. On the other hand, the correlation coefficients for the metallicity dependent transformations are larger than the ones of metallicity independent transformations indicating that the transformations actually vary with metallicity. The mean of the residuals, i.e. the color differences between those measured and those calculated, are smaller than 0.001 mag (except for the color $(r - J)$ which is equal to 0.001 mag). Additionally, the deviations of the measured colors from the calculated ones are absolutely smaller ($s \leq 0.16$) than the ones cited by Bilir et al. (2008) for dwarfs ($0.2 < s \leq 0.3$).

We applied our transformation equations to the synthetic BVI data of Pickles (1998) which cover stars of a wide spectral type range, and obtained $J - H$, $H - K_s$, $g - r$ and $r - i$ colors (Table 5) which gave us the chance to compare the two color diagrams in different studies. In all panels of Fig. 3, the grey circles correspond to the positions of our sample stars, whereas the dashed lines in panels (a), (b) and (c) represent the calibrations of Pickles (1998), Covey et al. (2008) and Straizys & Lazauskaite (2009), respectively. Finally, the continuous lines in panels (b) and (c) correspond to the two-color calibrations evaluated using the converted colors in Table 5. The deviation between the dashed and continuous lines in panel (b) originates from deviations of the positions of our sample stars from the synthetic $(B - V)$ and $(V - I)$ colors in panel (a). But the difference between two lines in panel (c) may be due to the uncertainty of the calibration itself, in addition to the mentioned deviations. However, we can argue that the transformations derived for late type giants in this work could be applied with sufficient accuracy.

5 Acknowledgments

We thank the anonymous referee for a thorough report and useful comments that helped in improving an early version

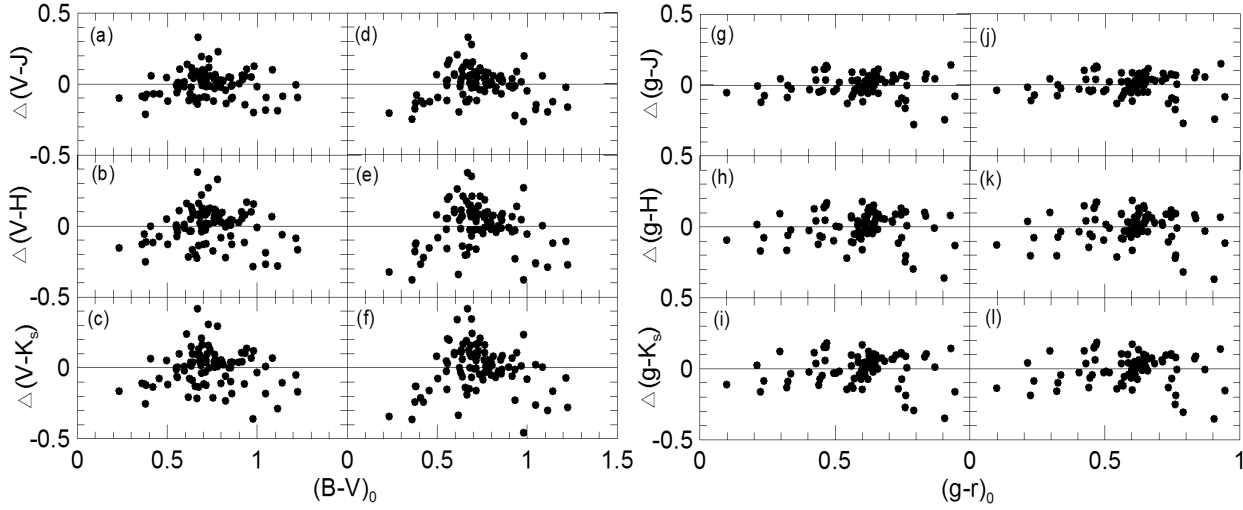


Fig. 5 Color residuals for two sets of transformations. The notation used is $\Delta(\text{color})=(\text{evaluated color})-(\text{measured color})$. The first and third columns correspond to the metal dependent transformations, whereas residuals for metallicity independent transformations are given in the second and fourth columns.

Table 3 Averages and standard deviations (s) for the residuals for different colors in transformation Eqs. (6)–(29). The notation used is $\Delta(\text{color})=(\text{measured color})-(\text{evaluated color})$.

For metallicity dependent transformation equations						
	$\Delta(B-J)$	$\Delta(V-J)$	$\Delta(I-J)$	$\Delta(g-J)$	$\Delta(r-J)$	$\Delta(i-J)$
Average	0.0007	0.0001	0.0006	0.0001	0.0010	-0.0004
s	0.142	0.089	0.077	0.106	0.073	0.069
	$\Delta(V-J)$	$\Delta(V-H)$	$\Delta(V-K_s)$	$\Delta(g-J)$	$\Delta(g-H)$	$\Delta(g-K_s)$
Average	0.0001	-0.0004	0.0002	-0.0007	0.0001	0.0002
s	0.097	0.133	0.133	0.081	0.110	0.108
For transformation equations independent from metallicity						
	$\Delta(B-J)$	$\Delta(V-J)$	$\Delta(I-J)$	$\Delta(g-J)$	$\Delta(r-J)$	$\Delta(i-J)$
Average	0.0003	0.0001	0.0001	0.0003	0.0001	0.0003
s	0.167	0.092	0.080	0.124	0.083	0.075
	$\Delta(V-J)$	$\Delta(V-H)$	$\Delta(V-K_s)$	$\Delta(g-J)$	$\Delta(g-H)$	$\Delta(g-K_s)$
Average	-0.0005	-0.0001	-0.0001	0.0004	-0.0001	-0.0005
s	0.113	0.160	0.162	0.081	0.110	0.108

Table 4 Synthetic data taken from Pickles' (1998) (columns 1-5) and $J-H$, $H-K_s$, $g-r$ and $r-i$ colors evaluated by the corresponding transformations derived in this work.

Spectral Type	$[M/H]$ (dex)	T_{eff} (K)	$B-V$	$V-I_c$	$J-H$	$H-K_s$	$g-r$	$r-i$
A0III	0	9572	0.037	0.008	-0.003	0.026	0.027	-0.050
A3III	0	8974	0.130	0.076	0.040	0.043	0.102	-0.019
A5III	0	8453	0.175	0.164	0.068	0.040	0.133	-0.006
A7III	0	8054	0.210	0.240	0.091	0.035	0.156	0.003
F0III	0	7586	0.271	0.317	0.123	0.040	0.202	0.022
F2III	0	6839	0.417	0.445	0.194	0.062	0.317	0.069
F5III	0	6531	0.425	0.507	0.204	0.052	0.318	0.069
G0III	-0.22	5610	0.661	0.726	0.330	0.086	0.509	0.149
G5III	-0.12	5164	0.886	0.872	0.428	0.131	0.690	0.223
G8III	0.06	5012	0.946	0.927	0.449	0.139	0.733	0.240
K0III	-0.08	4853	0.957	0.978	0.466	0.132	0.740	0.244
K1III	0.09	4656	1.036	1.044	0.496	0.145	0.800	0.268
K2III	0.05	4457	1.105	1.132	0.535	0.150	0.853	0.290
K3III	-0.02	4365	1.210	1.169	0.582	0.177	0.943	0.327

of the paper. S. Karaali is grateful to the Beykent University for financial support. This publication makes use of data products from the Two Micron All Sky Survey, which is a joint project of the University of Massachusetts and the Infrared Processing and Analysis Center/California Institute of Technology, funded by the National Aeronautics and Space Administration and the National Science Foundation.

This research has made use of the SIMBAD, NASA's Astrophysics Data System Bibliographic Services and the NASA/IPAC Extragalactic Database (NED) which is operated by the Jet Propulsion Laboratory, California Institute of Technology, under contract with the National Aeronautics and Space Administration.

References

- Abazajian K., Adelman-McCarthy J.K., Ageros M.A., Allam S.S., Anderson K., Anderson S.F., Annis J., Bahcall N.A., Baldry I.K., Bastian S., and 143 coauthors: 2004, *AJ* 128, 502
- Axer M., Fuhrmann K., Gehren T.: 1994, *A&A* 291, 895
- Bahcall J.N., Soneira R.M.: 1980, *ApJS* 44, 73
- Barbuy B., Erdelyi-Mendes M.: 1989, *A&A* 214, 239
- Bilir S., Ak S., Karaali S., Cabrera-Lavers A., Chonis T.S., Gaskell C.M.: 2008, *MNRAS* 384, 1178
- Burris D.L., Pilachowski C.A., Armandroff T.E., Sneden C., Cowan J.J., Roe H.: 2000, *ApJ* 544, 302
- Cabrera-Lavers A., González-Fernández C., Garzón F., Hammersley P. L., & López-Corredoira M.: 2008, *A&A* 491, 781
- Carney B.W., Wright J.S., Sneden C., Laird J.B., Aguilar L.A., Latham D.W.: 1997, *AJ* 114, 363
- Cavallo R.M., Pilachowski C.A., Rebolo R.: 1997, *PASP* 109, 226
- Cayrel de Strobel G., Soubiran C., Ralite N.: 2001, *A&A* 373, 159
- Chonis T.S., Gaskell C.M.: 2008, *AJ* 135, 264
- Clementini G., Gratton R.G., Carretta E., Sneden C.: 1999, *MNRAS* 302, 22
- Covey K.R., Hawley S.L., Bochanski J.J., West A.A., Reid I.N., Golimowski D.A., Davenport J.R.A., Henry T., Uomoto A., Holtzman J.A.: 2008, *AJ* 136, 1778
- Cutri R. M., Skrutskie M.F., Van Dyk S., Beichman C.A., Carpenter J.M., Chester T., Cambresy L., Evans T., Fowler J., Gizis J., Howard E., Huchra J., Jarrett T., Kopan E.L., Kirkpatrick J.D., Light R.M., Marsh K.A., McCallon H., Schneider S., Stiening R., Sykes M., Weinberg M., Wheaton W.A., Wheelock S., Zacarias N.: 2003, *2MASS All-Sky Catalog of Point Sources*, CDS/ADC Electronic Catalogues 2246
- Davenport J.R.A., Bochanski J.J., Covey K.R., Hawley S.L., West A.A., Schneider D.P.: 2007, *AJ* 134, 2430
- Dominy J.F.: 1984, *ApJS* 55, 27
- Drake J.J., Lambert D.L.: 1994, *ApJ* 435, 797
- ESA: 1997, *The Hipparcos and Tycho Catalogues* ESA SP-1200. ESA, Noordwijk
- Fan X.: 1999, *AJ* 117, 2528
- Fiorucci M., Munari U.: 2003, *A&A* 401, 781
- Fukugita M., Ichikawa T., Gunn J.E., Doi M., Shimasaku K., Schneider D.P.: 1996, *AJ* 111, 1748
- Fulbright J.P., Kraft R.P.: 1999, *AJ* 118, 527
- Fulbright J.P.: 2000, *AJ* 120, 1841
- Gilroy K.K., Sneden C., Pilachowski C.A., Cowan J.J.: 1988, *ApJ* 327, 298
- Gratton R.G.: 1983, *A&A* 123, 289
- Gratton R.G., Ortolani S.: 1984, *A&A* 137, 6
- Gratton R.G.: 1989, *A&A* 208, 171
- Gratton R.G., Sneden C.: 1991, *A&A* 241, 501
- Gratton R.G., Sneden C., Carretta E., Bragaglia A.: 2000, *A&A* 354, 169
- Gunn J.E., Carr M., Rockosi C., Sekiguchi M., Berry K., Elms B., de Haas E., Ivezić Z., Knapp G., Lupton R., and 30 coauthors: 1998, *AJ* 116, 3040
- Hogg D.W., Finkbeiner D.P., Schlegel D.J., Gunn J.E.: 2001, *AJ* 122, 2129
- Jordi K., Grebel E.K., Ammon K.: 2006, *A&A* 460, 339
- Karaali S., Bilir S., Tunçel S.: 2005, *PASA* 22, 24
- Kovacs N.: 1983, *A&A* 120, 21
- Kraft R.P., Sneden C., Langer G.E., Prosser C.F.: 1992, *AJ* 104, 645
- Krishnaswamy K., Sneden C.: 1985, *PASP* 97, 407
- Landolt A.U.: 1992, *AJ* 104, 340
- Leep E.M., Wallerstein G.: 1981, *MNRAS* 196, 543
- López-Corredoira M., Cabrera-Lavers A., Garzón F., & Hammersley P. L.: 2002, *A&A* 394, 883
- Lucas P.W., Hoare M.G., Longmore A., Schröder A.C., Davis C.J., Adamson A., Bandyopadhyay R.M., de Grijs R., Smith M., Gosling A., and 21 coauthors: 2008, *MNRAS* 391, 136
- Luck R.E., Bond H.E.: 1985, *ApJ* 292, 559
- Luck R.E., Bond H.E.: 1991, *ApJS* 77, 515
- Luck R.E., Wepfer G.G.: 1995, *AJ* 110, 2425
- Luck R.E., Challener S.L.: 1995, *AJ* 110, 2968
- Lupton R.H., Gunn J.E., Ivezić Z., Knapp G.R., Kent S., Yasuda N.: 2001, in *ASP Conf. Ser.: Astronomical Data Analysis Software and Systems X*, ed. F. R. Harden Jr., F.A. Primini and H.E. Payne, 238, 269
- Marshall D.J., Robin A.C., Reylé C., Schultheis M., Picaud S.: 2006, *A&A* 453, 635
- Mishenina T.V., Klochkova V.G., Panchuk V.E.: 1995, *A&AS* 109, 471
- Ofek E.O.: 2008, *PASP* 120, 1128
- Peterson R.C.: 1981, *ApJS* 45, 421
- Pickles A.J.: 1998, *PASP* 110, 863
- Pilachowski C.A., Sneden C., Kraft, Robert P.: 1996, *AJ* 111, 1689
- Rodgers C.T., Canterna R., Smith J.A., Pierce M.J., Tucker D.L.: 2006, *AJ* 132, 989
- Ryan S.G., Norris J.E., Bessell M.S.: 1991, *AJ* 102, 303
- Ryan S.G., Lambert D.L.: 1995, *AJ* 109, 2068
- Ryan S.G., Deliyannis C.P.: 1998, *ApJ* 500, 398

- Schlegel D.J., Finkbeiner D.P., Davis M.: 1998, ApJ 500, 525
- Shetrone M.D.: 1996, AJ 112, 1517
- Skrutskie M.F., Cutri R.M., Stiening R., Weinberg M.D., Schneider S., Carpenter J.M., Beichman C., Capps R., Chester T., Elias J., and 21 coauthors et al.: 2006, AJ 131, 1163
- Smith V.V., Lambert D.L.: 1986, ApJ 303, 226
- Smith J.A., Tucker D.L., Kent S., Richmond M.W., Fukugita M., Ichikawa T., Ichikawa S., Jorgensen A.M., Uomoto A., Gunn J.E.: 2002, AJ 123, 2121
- Smith J.A., Tucker D.L., Allam S.S., Ivezić Z., Yanny B., Gunn J.E., Knapp G.R., Eisenstein D., Finkbeiner D., Fukugita M.: 2007, The Future of Photometric, Spectrophotometric and Polarimetric Standardization, ASP Conference Series, Vol. 364, Edited by C. Sterken, San Francisco: Astronomical Society of the Pacific, p. 91
- Spite M., Spite F.: 1980, A&A 89, 118
- Spite M., Molaro P., Franco P., Spite F.: 1993, A&A 271L, 1
- Spite, M., Pasquini, L., Spite, F.: 1994, A&A 290, 217
- Straizys V., Lazauskaite R.: 2009, BaltA 18, 19
- Tomkin J., Lemke M., Lambert D.L., Sneden C.: 1992, AJ 104, 1568
- Tomkin J., Lambert D.L.: 1999, ApJ 523, 234
- Tucker D.L., Kent, S., Richmond, M.W., Annis, J., Smith, J.A., Allam, S.S., Rodgers, C.T., Stute, J.L., Adelman-McCarthy, J.K., Brinkmann, J., and 24 coauthors: 2006, AN 327, 821
- van Leeuwen F.: 2007, A&A 474, 653
- Walkowicz L.M., Hawley S.L., West A.A.: 2004, PASP 116, 1105
- West A.A., Walkowicz L.M., Hawley S.L.: 2005, PASP 117, 706
- Yadav R.K.S., Sagar R.: 2004, MNRAS 349, 1481
- York D.G., Adelman J., Anderson J.E.Jr., Anderson S.F., Annis J., Bahcall N.A., Bakken J.A., Barkhouser R., Bastian S., Berman E., and 134 coauthors: 2000, AJ 120, 1579